CORE
Metadata, citation and similar papers at core.ac.uk
Provided by Ulster University's Research Portal

Electrochemical and Solid-State Letters, **9** (3) A175-A178 (2006)
1099-0062/2006/9(3)/A175/4/$20.00 © The Electrochemical Society

Enhanced Electrochemical Properties of Arrayed CN_x Nanotubes Directly Grown on Ti-Buffered Silicon Substrates

Wei-Chuan Fang,[a] Chia-Liang Sun,[b] Jin-Hua Huang,[a] Li-Chyong Chen,[b,z] Oliver Chyan,[c,*] Kuei-Hsien Chen,[d] and P. Papakonstantinou[e]

[a]*Department of Materials Science and Engineering, Materials Science Center, National Tsing Hua University, Hsinchu 300, Taiwan*
[b]*Center for Condensed Matter Sciences, National Taiwan University, Taipei 106, Taiwan*
[c]*Department of Chemistry, University of North Texas, Denton, Texas 76203, USA*
[d]*Institute of Atomic and Molecular Sciences, Academia Sinica, Taipei, Taiwan*
[e]*School of Electrical and Mechanical Engineering, University of Ulster, Newtownabbey, County Antrim BT37 OQB, NI, United Kingdom*

The effects of a Ti buffer layer on structural and electrochemical properties of arrayed nitrogen-containing carbon nanotubes (CN_x NTs) directly grown on Si substrates have been investigated. Cyclic voltammograms using $Fe(CN)_6^{3-}/Fe(CN)_6^{4-}$ as redox couple were measured to study the electrochemical activities of CN_x NTs. The highest peak current density was achieved at an optimal Ti thickness of 20 nm owing to the good conductivity of $TiSi_2$ and high number density of NTs. Therefore, we have demonstrated the direct growth of aligned NTs on Ti-buffered Si with improved electrochemical activity that is believed to be suitable for advanced microsystem applications.
© 2006 The Electrochemical Society. [DOI: 10.1149/1.2166507] All rights reserved.

Manuscript submitted August 24, 2005; revised manuscript received November 30, 2005.
Available electronically January 18, 2006.

Over a wide range of properties and applications of carbon nanotubes (CNTs), the electrochemical (EC) aspects of CNTs have attracted much attention. Che et al. are among the first to demonstrate the successful utilization of carbon nanotubule membranes as electrodes in electrocatalytic applications.[1] Nugent et al. have shown superior EC reactivity of CNTs, which can be ascribed to their high local density of states induced by helicity and topological defects.[2] However, it should be emphasized that in the above-mentioned reports the CNTs needed to be attached to a copper wire with silver epoxy or placed onto the surface of a glassy carbon for EC measurement. On the basis of such traditional mixing and printing methods, it is difficult to meet an emergent demand for advanced electrochemical devices. Therefore, it is of practical value to integrate the CNTs into EC microsystems fabricated by well-developed Si technology.[3,4]

Recently, Koehne et al. have demonstrated the use of CNTs grown on Cr-buffered Si substrates as nanoelectrodes for DNA sensors.[5] However, the Cr itself cannot sustain possible corrosive environment in solutions, and it also exhibits a relatively low conductivity. In this work we present an EC platform with arrayed nitrogen-containing NTs (CN_x NTs) directly grown on Ti-buffered Si substrates with optimal current density and ideal Nerstian behavior. More importantly, the vertical alignment of CN_x NTs makes them suitable for subsequent fabrication processes to form composites for EC energy generation and storage. Moreover, taking into account the interfacial reaction during the CN_x NTs growth sequences, unlike more resistive chromium silicides ($CrSi_2$),[6] the resulting titanium silicide ($TiSi_2$) buffered layer has comparable conductivity to Ti and significantly enhances the electrochemical activity and stability of CN_x NTs.

Experimental

For the preparation of buffered Si substrates, Ti metal films with various thicknesses were deposited on n-type Si by electron-beam evaporation. Then the Fe thin film was deposited by ion beam sputtering deposition either on bare or Ti-buffered Si. Prior to CN_x NTs growth, hydrogen plasma treatment (2 kW, 10 min) was employed for generating Fe catalyst nanoparticles. Subsequently, the CN_x NTs were grown by microwave-plasma enhanced chemical-vapor deposition (MPECVD).[7] The reactive gas mixture was $CH_4/H_2/N_2$ with fixed flow rates of 20/80/80 sccm. The applied microwave power during the growth of CN_x NTs was 2 kW, the chamber pressure was adjusted to obtain a stable plasma, and the deposition time was kept at 10 min. For characterization, Raman spectra were measured in the backscattering geometry using the 514-nm line of an Nd:yttrium aluminum garnet (YAG) laser in the spectral range from 1000 to 2000 cm^{-1}. A JEOL 6700 field-emission scanning electron microscope (FESEM) was employed to examine the CN_x NTs morphologies and a Mac grazing incident X-ray diffractometer (GIXRD) was used to identify the phase of films. The electrical resistances of the films before and after MPECVD were determined by four-point probe measurements. In the latter cases, the electrical resistance was evaluated after the removal of NTs on substrates by boiling samples in a 6 M HNO_3 solution at 100°C for 1 h. Because titanium and titanium silicide[8] are chemically stable in nitric acid, the above procedure is believed not to affect their resistance. Electrical measurements were performed by standard four-point probe method wherein two probes were used to apply a fixed voltage V on the thin film and the other two were used to collect the current I. Sheet resistance was then calculated by $R_s = 4.53 \times (V/I)$. The EC measurements were carried out with a μ Autolab potentialstat/golvanostat type III system in a three-electrode configuration. The redox system employed here was 1 mM potassium ferricyanide $[K_3Fe(CN)_6]$ in 1 M H_2SO_4.

Results and Discussion

The Raman spectra were acquired for CN_x NTs grown on bare Si and Ti-buffered Si, in which the Ti thicknesses are varied from 20 to 200 nm. It is clear to observe that all three Raman spectra (not shown here) have similar D and G bands located approximately at 1350 and 1580 cm^{-1}, implying that the NTs have similar structures. In addition, the integrated intensity ratios of D and G bands (I_D/I_G) for all samples keep around the same value of 1.1, suggesting that the insertion of a Ti buffer layer would not influence the crystalline quality as well as the structure of NTs.

Figure 1 presents typical cross-sectional SEM micrographs of CN_x NTs grown on (a) bare Si, (b) Ti (20 nm)/Si, and (c) Ti (200 nm)/Si substrates, respectively. On bare the Si substrate the aligned CN_x NTs have the diameters of 5 to 30 nm and the length around 6 μm. In contrast, as shown in Fig. 1b and c, the morphologies of NTs change significantly with the Ti buffer layers on top of Si, though the NTs still remain quasi-aligned vertically to the Ti

* Electrochemical Society Active Member.
z E-mail: chenlc@ccms.ntu.edu.tw

Downloaded 07 Jan 2010 to 193.61.144.141. Redistribution subject to ECS license or copyright; see http://www.ecsdl.org/terms_use.jsp

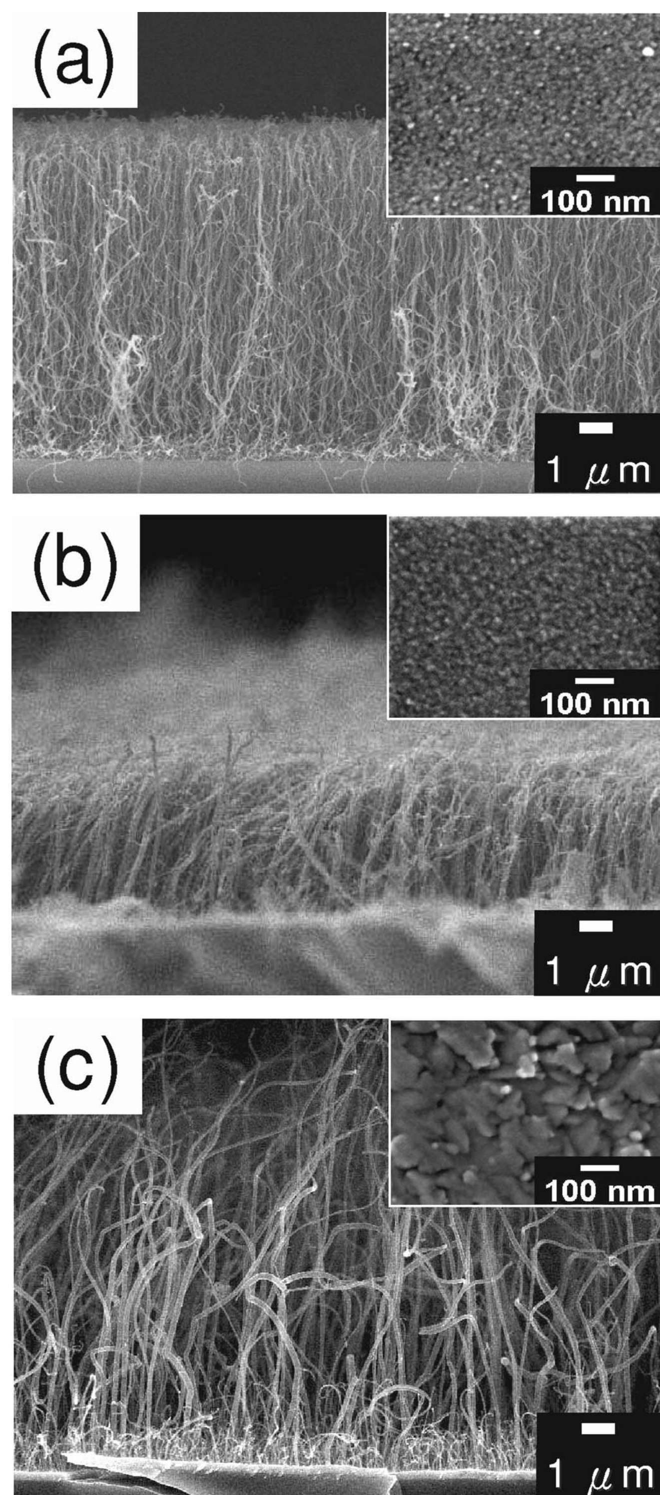

Figure 1. Cross-sectional SEM images of CN_x NTs on (a) bare Si, (b) Ti (20 nm)/Si, and (c) Ti (200 nm)/Si substrates. The insets are plan-view SEM images of the catalyst layer after a H_2 plasma treatment.

films. It is found that on 20-nm-thick Ti film the NTs length becomes shorter but on the thicker 200-nm Ti the NTs exhibit two distinct lengths, extremely long or short. In order to interpret this morphology evolution, we further take the top-view SEM images of Fe catalysts which are obtained after H_2-plasma treatment but before MPECVD. As illustrated in inset of Fig. 1c, it is obvious that the surface is covered predominantly by big (~100 nm) and irregular-shaped islands which are much different from the small (<10 nm) and circular ones typically found in Fig. 1a and b. The inhomogenous morphology of NTs can be attributed to the reaction of Ti and Fe during hydrogen plasma treatment that is able to form alloys[9] and thus affect the subsequent NTs growth.

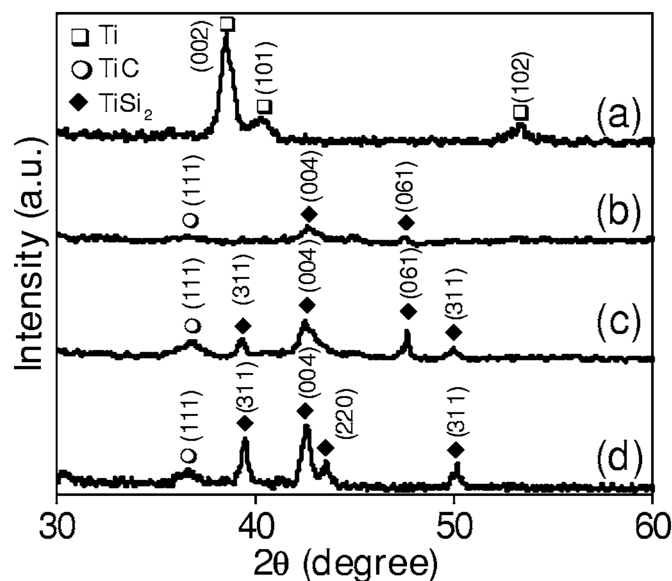

Figure 2. XRD patterns of (a) as-deposited Ti (200 nm)/Si and reaction layers of (b) Ti (20 nm)/Si, (c) Ti (50 nm)/Si, and (d) Ti (200 nm)/Si after MPECVD process.

Grazing incident X-ray diffraction (GIXRD) measurements of Ti-buffered Si before and after MPECVD were employed here in order to study the reactions among Ti, Si, and CN_x NTs. As displayed in Fig. 2a, there are three major peaks at 38, 40, and 53° for the as-deposited 200-nm-thick polycrystalline Ti film (JCPDS 05-0682). Surprisingly, all these Ti peaks disappear after MPECVD growth. With a very thin Ti layer (10 nm and data not shown here), nonstoichiometric silicides of Ti_5Si_4 and Ti_5Si_3 are formed. For the 20-nm-thick Ti case in Fig. 2b, the $TiSi_2$ phase is found to be generated (JCPDS 31-1405/10-0225), and it is worthwhile to mention that $TiSi_2$ is a widely used contact material because of its low resistivity and excellent chemical stability. In Fig. 2c and d, the $TiSi_2$ peaks become more obvious in thicker Ti films and the new peak at 36° is assigned to be (111) of TiC phase[10,11] (JCPDS 32-1383). Therefore, it suggests that the Ti film, acting as the current collector layer in EC measurements, would concurrently react with the bottom Si substrate as well as the top CNTs under the high-temperature MPECVD growth condition. On the other hand, the highly reductive hydrogen-plasma etching before MPECVD growth could effectively hinder TiO_2 formation.

The sheet resistances of the as-deposited Ti films and corresponding reaction layers formed after MPECVD are summarized in Fig. 3. For as-deposited Ti films, the apparent sheet resistances are ranged from 1,500 to 63(Ω/□). In general, the sheet resistance of the Ti film decreases with its thickness. Figure 3 also shows the resistances of reaction layers, see the black bars, transformed from Ti films after MPECVD. The sheet resistances before and after MPECVD process remain the same for 50, 200 nm thick films. In the case of 20-nm-thick Ti, the change in sheet resistance after MPECVD process is still negligible, whereas in the case of 10-nm-thick Ti, the resistance of its reaction layer is apparently much higher than its counterpart before MPECVD. Presumably, the formation of a continuous $TiSi_2$[12] layer in MPECVD cannot be achieved until the Ti thickness is over 20 nm. Once a continuous

Downloaded 07 Jan 2010 to 193.61.144.141. Redistribution subject to ECS license or copyright; see http://www.ecsdl.org/terms_use.jsp

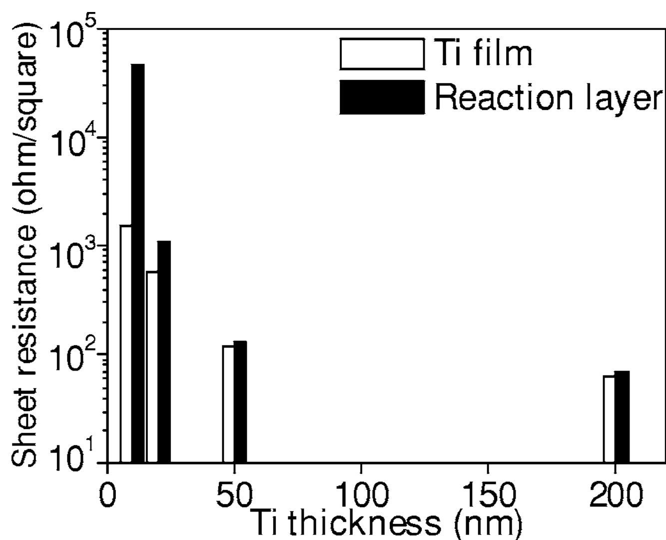

Figure 3. Sheet resistances as a function of Ti thickness before and after MPECVD process. The white bars are the resistances of Ti films and the black bars are those of the reaction layers after MPECVD.

layer of more conductive $TiSi_2$ is formed, the sheet resistances of this reacted layer could be comparable with that of metal Ti because of their similar resistivities.[13]

Figure 4a shows cyclic voltammograms (CVs) of CN_x NTs in the solution containing 1 M H_2SO_4/1 mM $K_3Fe(CN)_6$. It is noted that the highest current density is attained in the 20-nm-thick Ti case for all CN_x NTs directly grown on bare and Ti-coated Si. Despite the good conductivity of the $TiSi_2$ bottom current collector, it appears that other issues like the number density of NTs could also affect the EC activity. For thicker Ti samples, like 200 nm Ti in Fig. 1c, the less-dense and inhomogeneous morphology of CN_x NTs could result in reducing the effective electroactive area. As shown in Fig. 4b, a linear relationship between peak current (I_{pc}/I_{pa}) values and the root of scan rate ($\upsilon^{1/2}$) was observed at various scan rates for all samples, indicative of the heterogeneous electron transfer reactions limited by semi-infinite linear diffusion of $Fe(CN)_6^{3-}$ to the CN_x NTs electrode surface. Figure 4c shows the relationship of the peak potential separation (ΔE_p) and Ti thicknesses at a scanning rate of 5 mV/s. Following a similar trend as the resistances of reaction layers, the ΔE_p is much reduced in 20-nm-thick Ti sample and remains constant of ca. 60 mV for thicker Ti-buffered films. It suggests that the resistivity of the underlying conducting layer determines the reversibility, i.e., ΔE_p, of $Fe(CN)_6^{3-}/Fe(CN)_6^{4-}$ electron transfer process on CN_x NTs electrode surface when operated at the diffusion limited condition. Without any post-treatment, the improved ΔE_p of 60 mV from CN_x NTs on Ti buffered Si is close to the ideal value of 59 mV,[14] indicating that the NTs exhibit nearly reversible EC characteristics. It is clear that our aligned NTs on Ti-buffered Si are capable of fast electron transfer reaction, and the result is comparable to previous report in which they used silver paint to attach NTs on a copper electrode.[2] It is also noted that the addition of the Ti buffer layer can efficiently improve the adhesion of CN_x NTs with the Si substrate. The samples prepared as such remain mechanically intact and maintain stable EC performance.

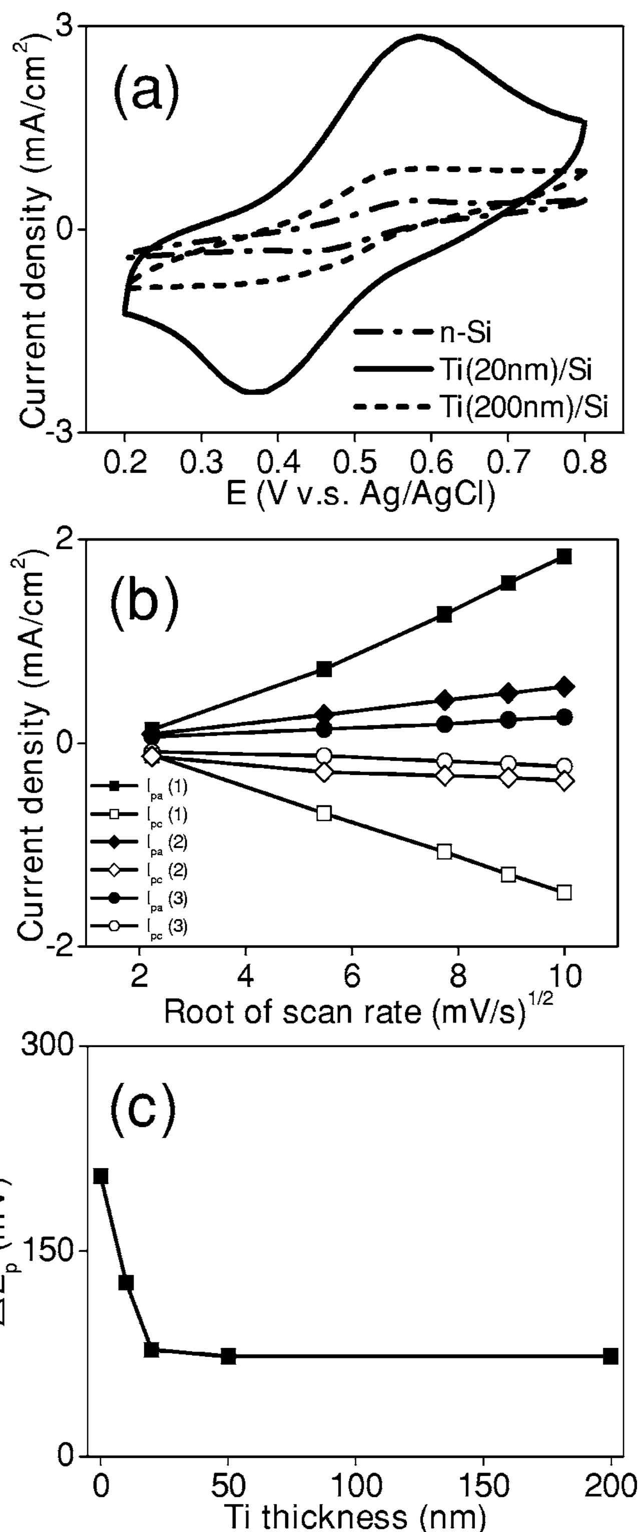

Figure 4. (a) Cyclic voltammograms of CN_x NTs at a scan rate of 100 mV/s in the solution comprising 1 M H_2SO_4 and 1 mM potassium ferricyanide. (b) The relationship between the peak current density and the root of the scan rate for CN_x NTs grown on (1) Ti (20 nm)/Si, (2) Ti (200 nm)/Si substrates, and (3) bare Si. I_{pa} and I_{pc} are the anode and cathode peak current density, respectively. (c) The ΔE_p as a function of Ti thicknesses at 5 mV/s.

Conclusions

In summary, we have demonstrated the enhanced EC performance of arrayed NTs on Si substrates by optimizing the thickness of the Ti buffer layer. The improved EC characteristics include increased current density by seven times and the nearly ideal reversibility for NTs on 20-nm-thick Ti film. Based on the similar Raman spectra signature, we conclude that the addition of a Ti buffer layer does not affect the structural quality of the NTs. The superior EC performance could be attributed to the high conductivity of $TiSi_2$ buffered layers as well as the high number density of NTs. There-

Downloaded 07 Jan 2010 to 193.61.144.141. Redistribution subject to ECS license or copyright; see http://www.ecsdl.org/terms_use.jsp

fore, our experimental results indicate that the aligned NTs on a Si-based platform with the aid of a Ti buffer layer would be suitable for future EC microsystem applications.

Acknowledgments

This work was supported by the National Science Council and Ministry of Education. O.C. acknowledges support from the Robert A. Welch Foundation.

L.-C. Chen assisted in meeting the publication costs of this article.

References

1. G. L. Che, B. B. Lakshmi, E. R. Fisher, and C. R. Martin, *Nature (London)*, **393**, 346 (1998).
2. J. M. Nugent, K. S. Santhanam, A. Rubio, and P. M. Ajayan, *Nano Lett.*, **1**, 87 (2001).
3. W. Ehrfeld, *Electrochim. Acta*, **48**, 2857 (2003).
4. C. L. Sun, L. C. Chen, M. C. Su, L. S. Hong, O. Chyan, C. Y. Hsu, K. H. Chen, T. F. Chang, and L. Chang, *Chem. Mater.*, **17**, 3749 (2005).
5. K. Koehne, J. Li, A. M. Cassell, H. Chen, Q. Ye, H. T. Ng, J. Han, and M. Meyyapan, *J. Mater. Chem.*, **4**, 676 (2004).
6. S. P. Murarka, *Silicides for VLSI Applications*, Academic Press, New York (1983).
7. L. C. Chen, C. Y. Wen, C. H. Liang, W. K. Hong, K. J. Chen, H. C. Cheng, C. S. Shen, C. T. Wu, and K. H. Chen, *Adv. Funct. Mater.*, **12**, 687 (2002).
8. V. Kolotyrkin, V. Knyazheva, O. Yurchenko, Y. Kolosvetov, and T. Stoyanovskaya, *Prot. Met.*, **28**, 418 (1992).
9. W. G. Moffat, *The Handbook of Binary Phase Diagrams*, Genium Publication Corporation, Schenectady, New York (1986).
10. Y. Zhang, T. Ichihashi, E. Landree, F. Nihey, and S. Iijima, *Science*, **285**, 1719 (1999).
11. R. Martel, V. Derycke, C. Lavoie, J. Appenzeller, K. K. Chan, J. Tersoff and Ph. Avouris, *Phys. Rev. Lett.*, **87**, 256805–1 (2001).
12. B. Herner, K. S. Jones, H. J. Gossmann, R. T. Tung, J. M. Poate, and H. S. Luftman, *J. Appl. Phys.*, **82**, 583 (1997).
13. T. G. Berlincourt, *Phys. Rev.*, **114**, 969 (1959).
14. P. T. Kissinger and W. R. Heineman, *Laboratory Techniques in Electrochemical Chemistry*, Marcel Dekker, Inc., New York (1996).

Downloaded 07 Jan 2010 to 193.61.144.141. Redistribution subject to ECS license or copyright; see http://www.ecsdl.org/terms_use.jsp